

Self-similar fluctuation and large deviation statistics in the shell model of turbulence

Yasuya Nakayama,¹ Takeshi Watanabe,² and Hirokazu Fujisaka¹

¹*Department of Applied Analysis and Complex Dynamical Systems, Graduate School of Informatics, Kyoto University, Kyoto 606-8501, Japan*

²*Division of Global Development Science, Graduate School of Science and Technology, Kobe University, Kobe 657-8501, Japan*
(Received 28 January 2001; published 24 October 2001)

Both static and dynamic multiscalings of fluctuations of energy flux and energy dissipation rate in the Gledzer-Ohkitani-Yamada (GOY) shell model of turbulence are numerically investigated. We compute the large deviation rate function of energy flux not only in the inertial range (IR) but also around the crossover between the inertial range and the dissipation range (DR). The rate function in IR exists to be concave, which assures the applicability of the Legendre transformation with the anomalous scaling exponents that have been investigated so far, and turns out to be independent of the Reynolds number. On the contrary, near the crossover scale, an intermediate dissipation range (IMDR) scaling is observed with the rate function in IMDR, which is accounted with the argument on dissipation scale fluctuation dominated by the energy flux fluctuation in the inertial range. Furthermore, to study the difference between IR intermittency and DR intermittency, we compute finite time-averaged quantities of energy flux and energy dissipation rate and investigate their multi-scaling behavior. The difference observed in terms of their dynamic multiscaling is discussed.

DOI: 10.1103/PhysRevE.64.056304

PACS number(s): 47.27.Gs, 02.50.-r, 05.40.-a, 47.27.Jv

I. INTRODUCTION

One of the most important problems in fully developed turbulence is the small-scale statistics of the energy transfer. The energy injected at the large-scale L transfers down to the dissipation scale η where the energy is dissipated into molecular motion due to viscosity. Universal statistics free from the viscous effect as well as mechanisms of energy injection is expected to hold in the range of length scale $\eta \ll l \ll L$, the so-called inertial range, provided that the Reynolds number is sufficiently large. In the inertial range, moments of suitable observables defined over the scale l show power-law dependence on l . In particular, the two quantities, the longitudinal velocity difference $\delta v_l \equiv [\mathbf{v}(\mathbf{x} + \mathbf{l}) - \mathbf{v}(\mathbf{x})] \cdot \mathbf{l}/l$ and the locally averaged energy dissipation rate ϵ_l averaged over a region of scale l , are mainly measured. These quantities are characterized by the scaling exponents $\zeta(q)$ and $\tau(q)$ defined as

$$\langle |\delta v_l|^q \rangle \sim V_0^q \left(\frac{l}{L} \right)^{\zeta(q)}, \quad \langle \epsilon_l^q \rangle \sim \epsilon_0^q \left(\frac{l}{L} \right)^{\tau(q)}, \quad (1.1)$$

where $\langle \cdot \rangle$ is the ensemble average, and V_0 and $\epsilon_0 (= \epsilon_L)$ represent the characteristic velocity and energy dissipation rate at scale L , respectively, which are assumed to exhibit no relevant fluctuation. From the definition (1.1), one finds that $\zeta(q)$ and $\tau(q)$ are convex functions of q .

In the Kolmogorov 1941 (K41) theory [1] it was supposed that relevant parameter on the small-scale statistics in fully developed turbulence is the energy-transfer rate and that the scaling exponent $\zeta_{K41}(q) = q/3$ was predicted via dimensional argument. However, $\zeta(q)$ by experimental measurement deviates from the K41 law, especially for large q [2]. This is called the anomalous scaling. The origin of the anomalous scaling is believed to be a strong intermittent fluctuation of the energy-transfer rate. To determine $\zeta(q)$ is thus called the intermittency problem. The energy-transfer

rate was treated as the constant parameter in K41 theory, and is expressed as the constant energy dissipation rate ϵ_l . The fluctuating energy-transfer rate can give the correction to the K41 scaling.

It is important to know the nature of energy-transfer fluctuation at scale l to study the intermittency problem. One relevant quantity is the energy flux. The energy flux at scale l represents the rate of nonlinear energy transfer from large to small scales per unit time through the scale l . Physically, the locally averaged energy dissipation rate ϵ_l may be thought to be equivalent to the energy flux. In the Kolmogorov 1962 theory (K62), the fluctuations of ϵ_l and the energy flux at a scale l were assumed to be fundamentally the same [3] in connection with the refined similarity hypothesis

$$\delta u_l \sim l^{1/3} \epsilon_l^{1/3}. \quad (1.2)$$

The combination of Eqs. (1.1) and (1.2) thus immediately leads to

$$\zeta(q) = q/3 + \tau(q/3). \quad (1.3)$$

The q th intermittency exponent $\tau(q)$ defined in Eq. (1.1) has been extensively investigated both numerically and experimentally [4–6]. The energy flux and the locally averaged energy dissipation rate are almost equal on the average, whereas it is not *a priori* known that their fluctuation natures are rigorously the same.

In this paper, we will discuss the intermittent fluctuation of the energy-transfer process of the Gledzer-Ohkitani-Yamada (GOY) shell model [7] by use of the large deviation-rate function, discussing overall statistics of exponent fluctuation relevant to the similarity characteristics of the energy-transfer process. We numerically solve the GOY shell model of the dynamical energy-cascade model of turbulence and compute the rate function of the energy flux. Moreover, we compare the fluctuations of the inertial range energy flux and the energy dissipation rate about their dynamic scaling.

In Sec. II, we develop the rate-function formalism to characterize the intermittency utilizing the large deviation theory. In Sec. III, we determine the rate function of the energy flux of the GOY model, numerically solving the dynamical equation for shell variables. It will turn out that in the inertial range, the rate function characterizes the energy-flux intermittency and near the dissipation scale it obeys different scaling than the inertial range by the effect of viscosity. In Sec. IV, we propose an approach to characterize the temporal fluctuation of the energy flux and energy dissipation rate by observing the statistics of their finite time averages. It will be found that the moments of their finite time averages obey power-law scaling, and then we discuss the difference between energy flux and energy dissipation observed in the scaling-exponent fluctuation. In Sec. V, one finds concluding remarks.

II. RATE-FUNCTION FORMALISM OF INTERMITTENCY

In this section, we review the rate-function formalism to characterize the intermittent statistics of energy transfer. The basic ideas are (1) the self-similarity hypothesis on fluctuations of different scales introduced first in the Kolmogorov 1962 (K62) theory [3], (2) the treatment of intermittent strong fluctuation by the large deviation theory (LDT) applied to the fluctuation of exponents of energy transfer [8–10,13].

For the locally averaged energy dissipation rate, $\epsilon_n \equiv \epsilon_{l_n} = \int_{|\mathbf{r}| < l_n} \epsilon(\mathbf{x} + \mathbf{r}) d\mathbf{r} / l_n^3$, with the scale $l_n = L\lambda^{-n}$, ($\lambda > 1$), the local scaling exponent z_n is introduced through $\epsilon_{n+1} / \epsilon_n = \lambda^{z_n}$. The fluctuation of ϵ_n is expressed using the finite average of z_n , $\bar{z}_n = \sum_{j=0}^{n-1} z_j / n$

$$\epsilon_n = \epsilon_0 \lambda^{n\bar{z}_n} = \epsilon_0 \left(\frac{L}{l_n} \right)^{\bar{z}_n}. \quad (2.1)$$

One may assume that ϵ_0 is constant since the fluctuation of the energy-dissipation rate at the largest scale L may be negligible compared to that at small scales. The self-similarity of the fluctuation of ϵ_n at each scale implies that the statistics of z_n is independent of n . For n sufficiently larger than the correlation step of z_j , LDT [8,11] may be applied to the probability density function (PDF) of \bar{z}_n , $Q_n(z) = \langle \delta(\bar{z}_n - z) \rangle$, that its asymptotic form takes $Q_n(z) \sim \sqrt{n} \exp_\lambda[-S(z)n]$, where $\exp_\lambda(x)$ denotes λ^x . Here, the function $S(z)$, being independent of n , is called the rate function, Cramér function [8], or the fluctuation spectrum [11], and characterizes the asymptotic form of PDF for \bar{z}_n fluctuation. Ergodicity assumption of z_n requires that $S(z)$ is concave and takes the minimum zero at $\langle z \rangle$. With the use of PDF $Q_n(z)$ for \bar{z}_n , PDF for ϵ_n is given by

$$P_{\epsilon_n}(\epsilon) \sim \frac{\epsilon^{-1}}{\sqrt{\ln(L/l_n)}} \exp_{L/l_n} \left[-S \left(\log_{L/l_n} \left(\frac{\epsilon}{\epsilon_L} \right) \right) \right]. \quad (2.2)$$

In the above consideration, $S(z)$ is a fundamental function in describing the self-similar energy cascade, and we expect

that these functions are universal characterizing the energy-cascade statistics in the inertial range in fully developed turbulence.

Next, the moments of ϵ_n are obtained as

$$\langle \epsilon_n^q \rangle \equiv \int_0^\infty \epsilon^q P_{\epsilon_n}(\epsilon) d\epsilon \propto \int_{-\infty}^\infty \exp_\lambda[-n(S(z) - qz)] dz. \quad (2.3)$$

The integral is evaluated by the steepest descent method for large n by supposing $S''(z) > 0$, which lead to

$$\tau(q) = \min_z [S(z) - qz]. \quad (2.4)$$

Thus $\tau(q)$ is related to the rate function $S(z)$ via the Legendre transformation. Equation (2.4) yields

$$\tau(q) = S(z(q)) - qz(q), \quad (2.5)$$

$$q = \frac{dS(z(q))}{dz}, \quad (2.6)$$

$$z(q) = -\frac{d\tau(q)}{dq}. \quad (2.7)$$

For the characterization of intermittent energy-transfer statistics, the q th order moment of ϵ_n gives the information of the fluctuation of z . Small z describes a weak fluctuation and strong intermittency is characterized by large z . The functional form of $S(z)$ is directly related to probabilities of various intermittent events of turbulent field and describes the overall features of intermittent fluctuation.

Let us here add a comment on estimating the maximum degree of order of moments $\langle \epsilon_n^q \rangle$ using the rate function. One always has a finite amount of data. This fact causes the problem of statistical convergence of moments $\langle \epsilon_n^q \rangle$. The moments with large q are determined mainly by the right tail of PDF $P_{\epsilon_n}(\epsilon)$ where the statistical accuracy is not sufficient enough. This implies that there exists a characteristic value q_{max} of q , for q smaller than q_{max} the statistical convergence of the moments is enough, but it is not sufficient for q larger than q_{max} . The characteristic value q_{max} may be evaluated as follows. Let ϵ_* be the boundary that separates the accuracy of the statistical convergence of PDF, i.e., PDF becomes unresolved at ϵ_* as ϵ is increased. The moments $\langle \epsilon_n^q \rangle$ for sufficiently large q are approximately proportional to ϵ_*^q . This means that $\tau(q)$ does linearly depends on q . The q -linear dependence of $\tau(q)$ thus results from the existence of the cutoff ϵ_* . By defining the characteristic exponent z_{max} by $\epsilon_* / \epsilon_0 = \lambda^{z_{max}}$, q_{max} is evaluated by the solution of $z(q_{max}) = z_{max}$, where the function $z(q)$ is the same as defined in Eq. (2.7) for $q \leq q_{max}$. The present estimation of q_{max} is alternative to the conventional one [2,12] where q_{max} is estimated by checking that the $\epsilon^q P_{\epsilon_n}(\epsilon)$ curve has a discernible peak and decays sufficiently fast as ϵ is increased. The rate function provides another way to estimate q_{max} .

Calculating $q(z)$ using Eq. (2.6), one may conveniently find q_{max} as the converged maximal $q(z)$. This data processing is achieved since the rate function directly describes the nature of the large fluctuation.

Let us turn to the discussion of the shape of $S(z)$. The central limit theorem (CLT) states that $S(z)$ parabolically depends on z near its minimum at $z = \langle z \rangle [= z(0)]$, thus, the K62 log-normal description may be correct near the minimum region of $S(z)$. However, beyond the range of the application of CLT, there is no reason for $S(z)$ to have a parabolic form that is a strong assumption used in K62 theory. Then one's interest goes to the determination of the shape of $S(z)$ in the range of large deviation from mean $\langle z \rangle$, i.e., of $z(q)$ for large $|q|$.

Hereafter, to analyze the intermittent energy-transfer statistics, we use a shell model for energy cascade of turbulence. Various types of shell models are so-far proposed [14]. We take here the so-called GOY model [7] and directly calculate $S(z)$ of energy flux by numerically integrating the dynamical equation and compare the results with theories so far proposed.

III. SELF-SIMILAR FLUCTUATIONS OF ENERGY-FLUX STRUCTURE FUNCTIONS

The GOY model [7] is written as

$$\frac{du_n}{dt} = ik_n \left(u_{n+1}^* u_{n+2}^* - \frac{1}{4} u_{n-1}^* u_{n+1}^* - \frac{1}{8} u_{n-1}^* u_{n-2}^* \right) - \nu k_n^2 u_n + \delta_{n,4} f. \quad (3.1)$$

Here, $k_n = k_0 \lambda^n$ ($n=1, \dots, N$) is the geometrically spaced wave number, $k_0 (= L^{-1})$ being taken as the smallest, characteristic wave number and u_n is a single complex variable of the shell-number n corresponding to the wave-number k_n ; ν is the kinematic viscosity and f is a constant forcing restricted on the fourth shell. For $\nu = f = 0$, the model conserves the total-energy $E = \sum_{n=1}^N |u_n|^2 / 2$. The parameters (ν, N) are chosen in a way the inertial range is well resolved. As reported in Refs. [7,14,15], the model displays intermittent dynamics and the velocity structure-function exponent $\zeta(q)$ defined by $\langle |u_n|^q \rangle \sim k_n^{-\zeta(q)}$ in the inertial range shows anomalous scaling, i.e., the scaling exponent is different from the K41 scaling law.

The energy equation in the GOY model takes the form

$$\frac{d}{dt} \frac{|u_n|^2}{2} = -\nu k_n^2 |u_n|^2 + \text{Re}[f u_n^* \delta_{n,4}] + F_{n-1} - F_n, \quad (3.2)$$

where

$$F_n = -k_n \text{Im} \left[u_n u_{n+1} u_{n+2} + \frac{1}{4} u_{n-1} u_n u_{n+1} \right] \quad (3.3)$$

is the energy flux from the n th shell to the $(n+1)$ -th shell that represents the nonlinear energy transfer on scale $1/k_n$. Summing up Eq. (3.2) in terms of shell indices gives

$$\frac{d}{dt} E = -\epsilon + \text{Re}[f u_4^*], \quad (3.4)$$

$$\epsilon = \nu \sum_{n=1}^N k_n^2 |u_n|^2. \quad (3.5)$$

The total energy E is thus dissipated at the rate ϵ .

In the K62 theory, the fluctuation of energy flux at a scale $l = 1/k$ is assumed to be the same as that of ϵ_l , which corresponds, in the present case, to $\epsilon_n \sim |F_n|$. In the GOY model, one may treat the energy-flux F_n at a scale $1/k_n$, one need not use the energy dissipation rate ϵ . By concerning the inertial range intermittency of the energy cascade, F_n has a clear physical meaning rather than u_n , therefore, hereafter we investigate the rate function for the energy-flux F_n . In the inertial range scale, we expect that the power-law

$$\langle |F_n|^q \rangle \sim k_n^{-\tau(q)} \quad (3.6)$$

and $\zeta(q) = q/3 + \tau(q/3)$ is established because of the scaling relation $|F_n| \sim k_n |u_n|^3$.

Hereafter, the rate function for the energy-flux F_n is calculated in two different ranges: (Sec. III A) the inertial range, where the long-time average of F_n is almost constant.; (Sec. III B) the intermediate dissipation range, which is near the crossover between the inertial and the dissipation ranges, although in the scale where the inertial range scaling gradually breaks, the multifractal phenomenology predicts that strong singularity associated with highly intermittent behavior still holds the inertial range scaling [16].

A. Inertial range case

In this section, we consider the intermittent fluctuation of the energy-flux F_n in the inertial range. Without loss of generality, we put $\lambda = 2$, and calculate the rate function $S(z)$ of $|F_n|$, which is numerically estimated from the PDF $Q_n(z)$ of

$$\bar{z}_n = \log \frac{|F_n|}{\langle |F_n| \rangle} \bigg/ \log \frac{k_n}{k_0} = (\log |F_n| - \log \langle |F_n| \rangle) / n \log 2$$

by

$$S_n(z) = -\frac{1}{n \log 2} \log [Q_n(z) / Q_n^M], \quad (3.7)$$

$$Q_n^M = \max_z Q_n(z). \quad (3.8)$$

$Q_n(z)$ is normalized by Q_n^M in such a way that $S(z)$ has the minimum zero. For sufficiently large n , $S_n(z)$ tends to $S(z)$, which is independent of n , and the value of z giving the minimum of $S(z)$ is equivalent to the long-time average value $\langle z \rangle$ of \bar{z}_n . However, we expect that due to the finiteness of n , the z value giving the maximum of $Q_n(z)$ is not equal to the mean value $\langle z \rangle$. Thus, for large but finite n , $\langle z \rangle$ is numerically determined by assuming $\langle \log |F_n| \rangle = \langle z \rangle n \log 2 + o(n)$. Then the function $S(z)$ is estimated by slightly shifting $S_n(z)$ along the abscissa so that the zero point is located

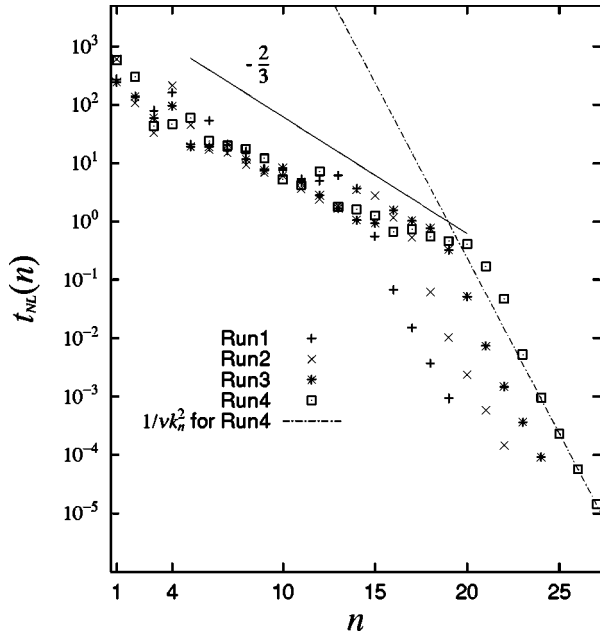


FIG. 1. Nonlinear time scales estimated as $t_{NL}(n) = \sqrt{\langle |u_n / (\dot{u}_n)_{NL}|^2 \rangle}$ for different runs, where $(\dot{u}_n)_{NL}$ is the nonlinear term in Eq. (3.1). The solid line shows the slope $-2/3$. The dash-dotted line shows the linear damping time scale for run 4.

at $\langle z \rangle$. One should note that in terms of $S(z)$, the PDF for $|F_n|$ is asymptotically given by

$$P(|F_n|) = \frac{Q_n^M |F_n|^{-1}}{\sqrt{\ln(k_n/k_0)}} \exp_{k_n/k_0} \left[-S \left(\frac{\ln(|F_n|/\langle |F_n| \rangle)}{\ln(k_n/k_0)} \right) \right]. \quad (3.9)$$

For the numerical integration of Eq. (3.1), the slaved-frog second-order Adams-Bashforth scheme [14,17] is used. The time increment Δt is chosen as follows. First, we carried out a preliminary calculation of characteristic time scales associated with shells of wave-numbers k_n 's using the fourth-order Runge-Kutta scheme. Next, we choose the time increment for the slaved scheme. The slaved scheme treats the linear term exactly and discretizes the nonlinear term integration. In the GOY model, there are two different characteristic time scales in each shell. One is the linear damping time scale $(\nu k_n^2)^{-1}$ and the other is due to the nonlinear term. For a high shell-mode n , the linear damping is dominant since νk_n^2 is large. In the inertial range, on the contrary, the nonlinear term dominates the dynamics and linear damping is weakly contributed. To trace the dynamics of an inertial range shell, one must choose Δt at least smaller than the smallest inertial range time scale. A nonlinear time scale numerically estimated is shown in Fig. 1. Figure 1 gives the guideline to choose the integration time increment Δt , which is chosen sufficiently small in comparison with the smallest time scale among all shell modes. Thus, the energy-flux dynamics in the inertial range may be well traced as well as the energy dissipation rate dynamics. The parameters for numerical calculations are chosen as $k_0 = 2^{-4}$ and $f = 5.0(1+i) \times 10^{-3}$

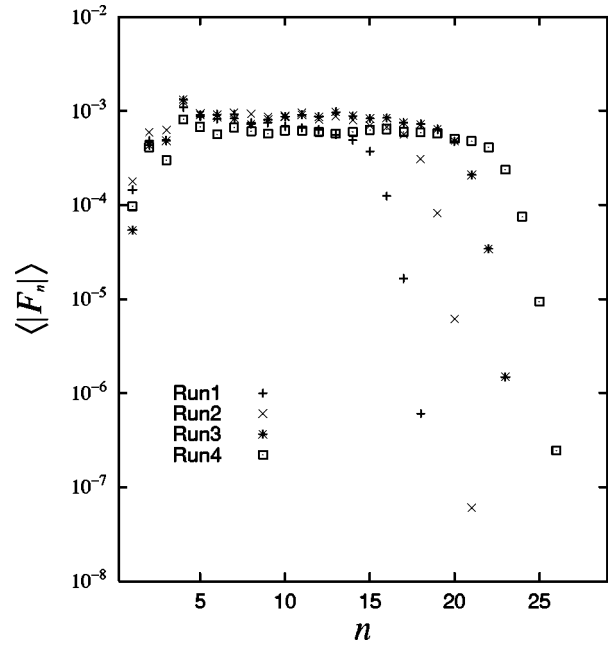


FIG. 2. Time averages of the moduli of energy fluxes for different runs.

with the total shell number $N=19$, $\nu=10^{-6}$ (run 1), $N=22$, $\nu=10^{-7}$ (run 2), $N=24$, $\nu=10^{-8}$ (run 3) and $N=27$, $\nu=10^{-9}$ (run 4).

In Fig. 2, we show the long-time average of $|F_n|$. One may recognize the existence of the inertial range where $\langle |F_n| \rangle$ is almost a constant irrespective of n . In Fig. 3, we show typical time series of $F_n(t)$ in the inertial range shells $n=15, 17, 19$ for run 4. One observes episodes of strong fluctuations in quiescent laminar phases, which represent intermittent energy-cascade transfer from large to small scales. Furthermore, one sees that the intensity of intermittent fluctuation becomes stronger in high wave-number shells. This figure suggests the existence of characteristics of the energy flux.

Figure 4 shows the rate function obtained by measuring $Q_n(z)$ for the energy-flux fluctuation for shells corresponding to the inertial range in run 4. One finds that $S_n(z)$ for different shell numbers are on the same curve. The converging function is the rate function $S(z)$. It is expected that $S(z)$ is the universal function characterizing the intermittent energy-cascade dynamics and is the same as in Eq. (2.2). It should be noted that the observed $S(z)$ is concave in its wide region. This concavity property guarantees the applicability of the Legendre transformation Eq. (2.4), which connects $S(z)$ and the q th intermittency exponent $\tau(q)$.

Let us make a remark on the shape of $S(z)$ on the left side where $S(z)$ approximately takes the form $S(z) = -a(z - z_m)$ with constants a and z_m . Inserting this into Eq. (3.9), one finds that the PDF of $|F_n|$ is represented as $P(|F_n|) \sim |F_n|^{a-1}$ in this region. The numerical result shows that a is about unity, which implies that PDF of $|F_n|$ is finite near $|F_n|=0$. This fact may be due to the existence of the inverse energy-cascade process, which means that F_n may become negative in some times. This nature is quite different from

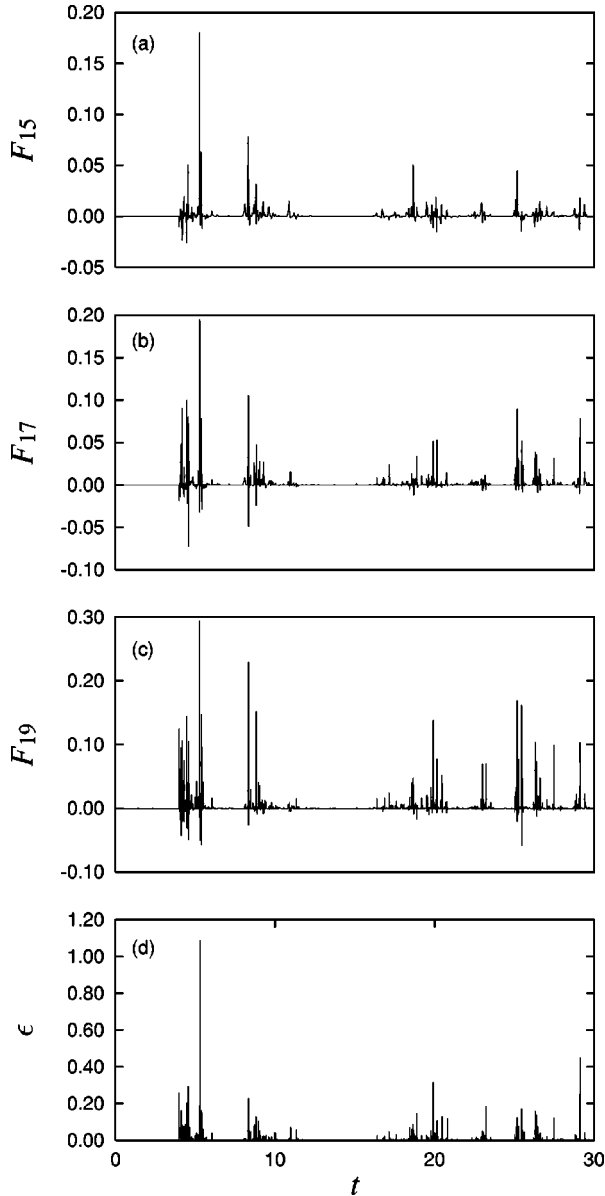


FIG. 3. Typical time evolutions of energy fluxes in the inertial range (a) $n=15$, (b) 17, and in the intermediate dissipation range (c) $n=19$, and of the energy dissipation rate (d) for run 4.

that of the energy dissipation rate which is a positive definite variable. So we expect that $S(z)$ for the energy dissipation rate takes different forms in its left branch than that of the present case. Let us consider the effect of this shape of PDF near the origin $|F_n|=0$ on moments of $|F_n|$. The contribution from the range $[0, \delta]$ to moments is estimated as

$$\langle |F_n|^q \rangle_\delta \sim \int_0^\delta x^{a-1} x^q dx, \quad (3.10)$$

for $\delta \ll 1$. This expression diverges for $q < -a$ and converges for $q > -a$ in the limit $\delta \rightarrow 0$, which means that moments of $|F_n|$ exist for $q > -a$ and $\tau(q)$ have its support in $q > -a$. This fact is easily recognized by noticing Eq. (2.6). The lower bound of the derivative of $S(z)$ is thus $a = -q_{min}$.

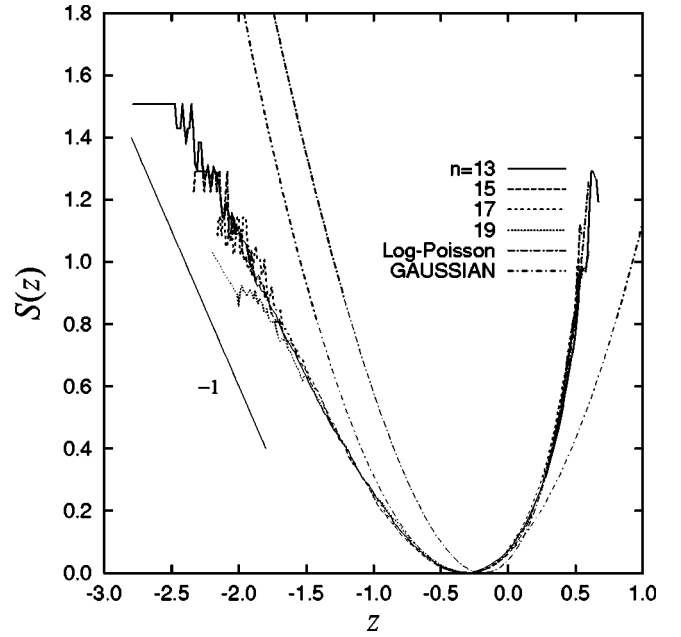


FIG. 4. Rate functions of energy flux in shells in the inertial range for run 4. The Legendre transformation of the She-Lévêque model (log-Poisson model) [Eq. (3.13)] with $\gamma=0.625$ and $d_0=1.48$, and the Gaussian approximation [Eq. (3.11)] are drawn for comparison. The straight line shows slope -1 .

In Fig. 4, we also show the comparison with some theoretical results based on different theoretical models. The CLT states that $S(z)$ around its minimum takes the parabolic form

$$S(z) \approx \frac{1}{|2\tau''(0)|} [z - z(0)]^2. \quad (3.11)$$

This gives the Gaussian form near the minimum of $S(z)$. Equivalently, we obtain $\tau(q) = \tau'(0)q + 1/2\tau''(0)q^2$. This approximation is valid only in the region where CLT is applicable, i.e., for appropriately small $|q|$. $S(z)$ is well fitted by this approximation around $z(0)$, but generally deviates from Eq. (3.11) for a large $|z - \langle z \rangle|$ region. This in general requires other statistics instead of the Gaussian statistics for strong, as well as weak fluctuations of z . Once one applies the form Eq. (3.11) to the whole region of z , the relation $z(0) = \tau''(0)/2$ is required by $\tau(1) = 0$ and this approximation is identical to the K62 log-normal model. In the K62 model, the intermittency exponent is given by $\mu = -\tau''(0) = -\tau(2)$, which is the only parameter characterizing $S(z)$ as well as $\tau(q) = -(\mu/2)q(q-1)$. In general, there is no reason to connect $z(0)$ and $-\tau''(0)$. The log-normal approximation can thus be applied to the fluctuation statistics around $z(0)$. One should be cautious that when defining $\mu = -\tau(2)$, not $-\tau''(0)$, the K62 log-normal model should be fitted around $z(2)$ but not $z(0)$. The present numerical study shown in Fig. 4 gives $z(0) = \langle z \rangle = -0.28$ and $-\tau''(0)/2 = 1/[2S''(\langle z \rangle)] = 0.30$. The observed values are apparently different from the prediction of K62. It should be

noted that the log-normal approximation is valid for moments with q satisfying $|z(q) - \langle z \rangle| \lesssim \sqrt{\tau''(0)}$. In the present case, this region is about $0 \leq q \leq 1$.

Next, we compare the numerical results to the phenomenological model by She and Lévéque (SL) [18]. This model is known to fit well the experimental $\zeta(q)$ and $\tau(q)$ for large q and so do the result of the GOY model [5,14,19]. The random cascade model (2.1) with the specific Poisson statistics on z_n yields the SL model, and the SL model is thus recognized as the log-Poisson model [20]. The q th intermittency exponent by the SL model and the rate function are obtained as

$$\tau_{SL}(q) = -\gamma q + d_0(1 - \beta^q), \quad d_0 = \frac{\gamma}{1 - \beta}, \quad (3.12)$$

$$S_{SL}(z) = \frac{z - \gamma}{\ln \beta} \left[\ln \left(\frac{z - \gamma}{d_0 \ln \beta} \right) - 1 \right] + d_0, \quad (3.13)$$

$$0 < \gamma \leq 3, \quad \gamma \leq d_0.$$

γ and d_0 are the same as $z(\infty)$ and $S[z(\infty)]$, respectively. The SL model is parametrized at the point $z(q \rightarrow \infty)$ that is of the strongest fluctuation, which means that the SL model should be compared with $\tau(q)$ in large q region or with $S(z)$ for $z > \langle z \rangle$ region. A large q picks out the strong intermittent fluctuation statistics. For the intermittency of the GOY model, these two parameters are numerically obtained by Lévéque and She [19] as $\gamma = 0.625$ and $d_0 = 1.48$ by using Eq. (3.12). The comparison of $S_{SL}(z)$ with these parameter values with the present numerical result is made in Fig. 4. One may find a good agreement in the right region of $S(z)$, where strong fluctuation is dominant, but not in the left region of weak fluctuation. One observes that $z(q)$ of large- q fluctuation coincides well with the SL model. This fact may be seen as a natural result since the SL model is regarded as the model explaining the strongest fluctuation and somehow extrapolates to the region near $z(q=0) = \langle z \rangle$ point, which was discussed in Ref. [21]. The SL model thus captures a strong fluctuation nature of intermittency in turbulence and it cannot be applicable for weak fluctuation. This feature of the SL model agrees with the result of direct numerical simulation of the Navier-Stokes equation [6] and the data analysis of real turbulent flow [5].

The inertial range intermittency is considered to be universal for turbulence at sufficiently large Reynolds number Re . In Fig. 5, we show converged rate functions for different runs in their inertial ranges. The results clearly show that converged rate functions are independent of Re .

We discuss some important quantities characterizing the universal statistics of intermittency in fully developed turbulence from the LDT viewpoint. $S(z)$ may be a universal function for a sufficiently large Reynolds number. The shape of $S(z)$ around the minimum is characterized by the two parameters $z(0)$ and $\tau''(0)$, which is an immediate result of the CLT. If $S(z)$ is well defined for $Re \rightarrow \infty$, $z(0)$ and $\tau''(0)$ are important quantities concerning small fluctuation around $z(0)$, and determine small $|q|$ behaviors of $\zeta(q)$ or $\tau(q)$. The intermittency exponent μ is well known as a universal

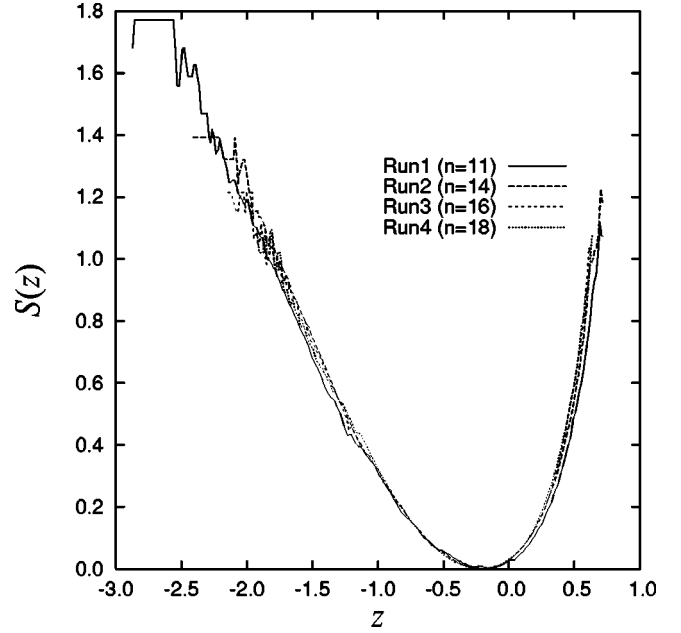


FIG. 5. Rate functions of the energy flux in the inertial range for different Reynolds numbers, $n=11$ for run 1, 14 for run 2, 16 for run 3, and 18 for run 4.

quantity characterizing intermittency. However, there is no particular reason that μ has a special role from the LDT viewpoint. Instead, $z(0)$ and $\tau''(0)$ are more important than μ to investigate the universal statistics of intermittency in turbulence.

Concerning large fluctuation, the SL model yields a good approximation of the observed $S(z)$. The SL model generally contains two parameters, i.e., γ and d_0 in Eq. (3.13). As stated above, these parameters determine the asymptotics of $S(z)$ near the largest z , i.e., the right edge of the $S(z)$ curve. They have great importance to characterize large fluctuation statistics. However, it is difficult to evaluate these parameters from experimental data because the amount of experimental data is always finite and the maximal value of z is just a maximum of sample data. On the other hand, one may construct a model of intermittency without the upper cutoff of z . The K62 log-normal model is an example of this kind. The possibility of the existence of γ and d_0 may be discussed as follows. As far as concerning energy dissipation multifractal in real turbulence, the exponent z is bounded, which is argued by the Novikov inequality [8,22]

$$\tau(q) \geq -3q \quad \text{for } (q \geq 0), \quad \tau(q) \leq -3q \quad \text{for } (q \leq 0). \quad (3.14)$$

This may give the large q asymptotic of $\tau(q)$ as

$$\tau(q) = -\gamma q + o(q), \quad q \rightarrow \infty, \quad (3.15)$$

thus, $z(q) = -\tau'(q)$ is bounded by γ [21]. For the GOY model, Lévéque and She [19] have done a detailed numerical measurement on the inertial range statistics of the modulus of $\Pi_n = (u_{n-1}u_nu_{n+1})^{1/3}$, and found there exists a maximum for the fluctuation of Π_n . These facts on real turbulence

and the GOY model suggest that to know γ and d_0 is quite important to treat large fluctuation on inertial range statistics.

B. Intermediate dissipation range case

In this section, we focus on the self-similarity around the crossover between the inertial and the dissipation ranges. In this crossover range, a scaling law different from that in the inertial range is observed as is predicted by the multifractal in the inertial range. This scale range is called as the intermediate dissipation range [16].

The key idea of the intermediate dissipation range is the fluctuation of the viscous cut-off scale and to relate it with the inertial range scaling. In the K41 theory, the viscous cutoff wave number is uniquely defined as $k_d = (\epsilon_0/\nu^3)^{1/4}$, so that the corresponding local Reynolds number is of order one. At this characteristic wave number, the dissipation starts to dominate. For wave-number k smaller than k_d , the inertial range scaling holds. On the other hand, in the multifractal description, the viscous cutoff is a fluctuating quantity due to a fluctuating energy transfer [16,23]. If we define the local Reynolds number by the energy transfer quantity ϵ_n at the scale $1/k_n$ as

$$\text{Re}_n = \frac{\epsilon_n^{1/3}}{k_n^{4/3} \nu}, \quad (3.16)$$

ϵ_n being characterized by the local scaling exponent z as $\epsilon_n \sim \epsilon_0 (k_n/k_0)^z$ [Eq. (2.1)], then one may estimate the z -dependent viscous cutoff $k_d(z)$ from Eq. (3.16) with $\text{Re}_n \sim 1$ as

$$\frac{k_d(z)}{k_0} \sim \left\{ \left(\frac{\epsilon_0}{k_0^4} \right)^{1/3} \frac{1}{\nu} \right\}^{3/(4-z)} \sim \text{Re}_0^{3/(4-z)} = \text{Re}^{3/(4-z)}. \quad (3.17)$$

In a fully developed turbulence ($\text{Re} \gg 1$), a larger z gives a smaller cutoff scale $1/k_d(z)$. This implies that the width of the inertial range scaling of $z(q)$ fluctuation is wider for larger $z(q)$; a higher-order structure function holds the inertial range scaling down to a smaller scale. In the language of the rate function $S_n(z)$ at those scales where the viscosity begins to affect, the shape of $S_n(z)$ starts to decline for small z . For large z of strong fluctuation, the shape of $S_n(z)$ is expected to still reserve as the inertial range shape. This scale range is the intermediate dissipation range.

We are interested in how the characteristic function $S_n(z)$ in this crossover range differs from the inertial range rate function $S(z)$, i.e., how $S_n(z)$ depends on n in this range. In the GOY model, this crossover range is located around the shell of the K41 viscous cutoff wave-number $k_\eta = 1/\eta$. The shell number corresponding to k_η is estimated as $k_\eta = (\epsilon_0/\nu^3)^{1/4} \equiv k_0 2^{n_d}$. The n_d 's for the present runs are summarized in Table I. It is seen in Fig. 2 that these n_d 's are approximately equal to the end of the inertial range. We compute the rate function $S_n(z)$ for shells around n_d , which should have the n dependence and differ from $S(z)$ in the inertial range.

TABLE I. Kolmogorov dissipation shell numbers $n_d \sim \frac{1}{4} \log_2(\epsilon_0/\nu^3)$, D value in Eq. (3.20), and $\log_2 \text{Re}$. ϵ_0 is order of 10^{-3} for all runs.

	Run 1	Run 2	Run 3	Run 4
n_d	12.5	14.9	17.4	19.9
D	0.94	0.97	0.97	0.96
$\log_2 \text{Re}$	21.95	25.39	28.73	31.89

The prescription to estimate $S_n(z)$ is applied to shells with wave numbers higher than those of the inertial range. In Fig. 6, we show the result for run 4. Compared with the inertial range $S(z)$, one finds the $S_n(z)$ curve coincides partially with the inertial range $S(z)$ in a large z region but differs than that for small z . This result agrees with the above discussion based on the multifractal description. In this crossover range, the inertial range scaling holds for large fluctuation of F_n but not for small F_n because of the viscous effect. This scaling is different from that of the inertial range and is characteristic of the intermediate dissipation range. The intermediate dissipation range scaling is qualitatively characterized by observing how $S_n(z)$ depends on the shell number n . The left wing slope of $S_n(z)$ becomes looser as n is larger, which means the probability of laminar state becomes larger and the energy flux is more intermittent than in the inertial range.

The z -dependent cutoff $k_d(z)$ is determined by Eq. (3.17). We will estimate the inverse function of $k_d(z)$, denoting $z_{k_n} = z_n$, utilizing the characteristic function $S_n(z)$ in the intermediate dissipation range of the data of Fig. 6. By supposing z is distributed over $[z_{\min}, z_{\max}]$, the intermediate dissipation range ranges over $k_d(z_{\min}) < k < k_d(z_{\max})$. For $k = k_n$ in this range, $1/k_n$ is a cutoff scale for z_n fluctuation and z_n is

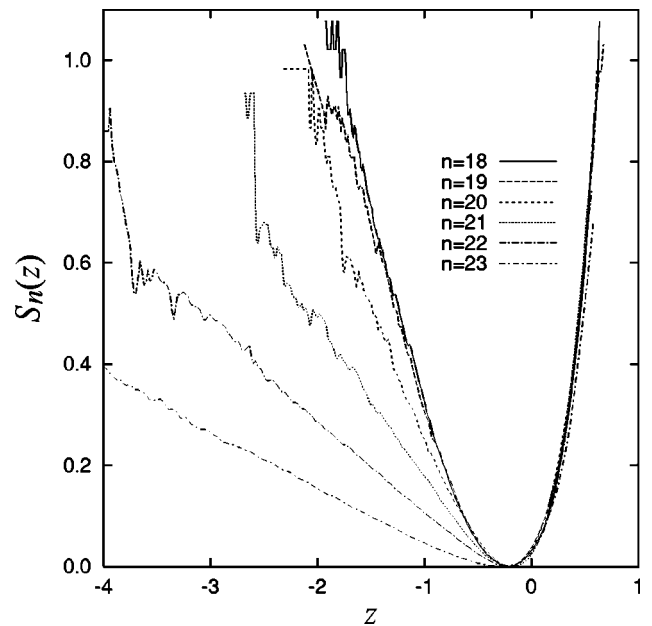


FIG. 6. Rate functions $S_n(z)$ of energy flux in the intermediate dissipation range $n = 18, \dots, 23$ for run 4.

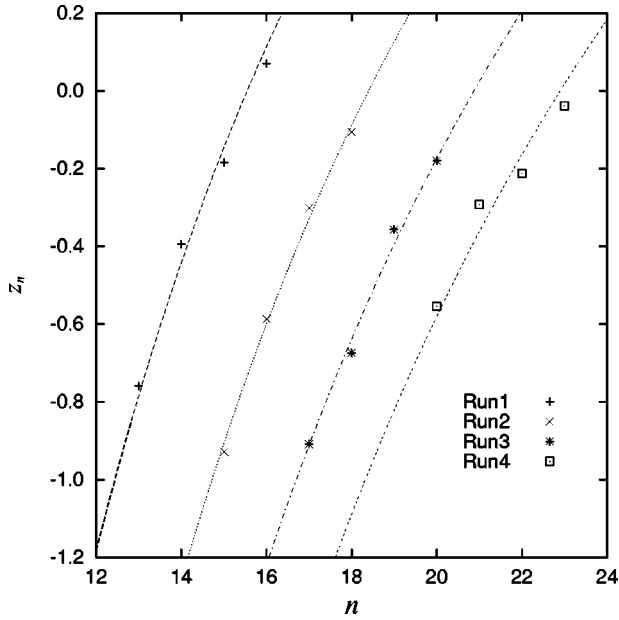


FIG. 7. Viscous cutoff scale exponent z_n for different runs. The inertial range scaling of z_n stops at the corresponding n . Fitting line [Eq. (3.19)] for each data is also shown.

identified with the smallest z where $S_n(z)$ coincides with $S(z)$. The z_n can be determined by comparing $S_n(z)$ and $S(z)$. In the intermediate dissipation range, the quantity $\nu(k_n/k_0)^{(4-z_n)/3} = \nu 2^{c_n}$ from Eq. (3.17) should become the same order irrespective of n , where $k_n = k_0 2^n$ and

$$c_n \equiv n \frac{4 - z_n}{3}. \quad (3.18)$$

We require that the exponent c_n is independent of n in the intermediate dissipation range. The n dependence of z_n is determined from Eq. (3.18) with $c_n = c$ as

$$z_n = 4 - \frac{3c}{n}. \quad (3.19)$$

How is the exponent c determined? From Eq. (3.17), c is determined by Re of the mean energy dissipation rate ϵ_0 as

$$c = D \log_2 \text{Re}, \quad (3.20)$$

where D is the coefficient of order one expected to be constant for high Re .

We determine z_n from the data shown in Fig. 6, and then plot z_n in Fig. 7. In Fig. 7, z_n is fitted to Eq. (3.19) by the least mean-square method. The numerical values of z_n 's are determined from data as the points at which the difference $d(z) = S(z) - S_n(z)$ crosses a given threshold δ . We regard $S_n(z)$ coincides with $S(z)$ if $d(z) < \delta$, and does not otherwise. The form (3.19) with a single parameter $c = c_\delta$, c_δ being the value of c for a given δ , seems to fit the data well. For reference, the value of c_δ for $\delta = 0.001$ for run 4 is 30.54. The functional form (3.19) is valid with properly small threshold δ , the fitting parameters c_δ 's are insensitive to the choice of δ as far as it is properly small.

The coefficient D in Eq. (3.20) for different runs are calculated with the fitting value c_δ and Re , and are summarized in Table I. It turns out that D is almost constant for runs. The values of $\log_2 \text{Re}$ are also shown in Table I for reference.

The results show that in the GOY model, the intermediate dissipation range scaling holds quite well. The z dependence of the viscous cutoff $k_\eta(z)$ is directly observed by use of $S_n(z)$. The inertial range multifractal leads to multicutoffs. This is quite a nature of complexity of turbulence.

In a fully developed turbulence, the cutoff scale is determined by the balance between nonlinear and viscous terms. In other words, this characteristic scale is determined by the competition between the energy flux and the energy dissipation. Since the energy flux exhibits strong, intermittent fluctuations, the cut-off scale also fluctuates. When the energy flux is active and becomes large, the cutoff scale η becomes smaller, and therefore, the inertial motion reaches a smaller scale, but on the contrary and when the energy flux is inactive and takes small value, η becomes larger. This situation may correspond to the case for real turbulent flow because the fluctuation is nonuniform spatially and temporally. The cutoff scale η thus will exhibit fluctuation according to the local amplitude of the energy flux, and the intermediate dissipation range scaling around the Kolmogorov scale η will be examined by observing the rate function.

IV. SELF SIMILARITY OF TIME CORRELATORS

In this section, we compare the fluctuation characteristics of the energy flux with those of the energy dissipation rate. An energy flux represents nonlinear energy transfer at a certain scale. In a fully developed turbulence, its average in the inertial range is almost constant irrespective of the wave number and takes the same order as the average energy dissipation rate. Thus, the K62 theory assumes that their fluctuation statistics are fundamentally the same as each other. However, the energy dissipation rate is the quantity characterizing dissipation range dynamics, and its fluctuation nature is not exactly the same as the energy flux fluctuation. To compare their fluctuation natures in the GOY model, we will consider their time averages and study their multiscaling characteristics.

For the energy flux F_n on a k_n shell and the energy dissipation rate ϵ we introduce their finite time averages over a time span t ,

$$|F_n|_t = \frac{1}{t} \int_{t_0}^{t_0+t} |F_n(s)| ds, \quad \epsilon_t = \frac{1}{t} \int_{t_0}^{t_0+t} \epsilon(s) ds. \quad (4.1)$$

Depending on t_0 , $|F_n|_t$ and ϵ_t are fluctuating quantities. For both quantities, multiscaling behavior is expected to hold in the sense that their moments obey

$$\langle |F_n|_t^q \rangle \sim t^{\tilde{\tau}_n(q)}, \quad \langle \epsilon_t^q \rangle \sim t^{\tilde{\tau}_\epsilon(q)}, \quad (4.2)$$

with characteristic functions $\tilde{\tau}_n(q)$ and $\tilde{\tau}_\epsilon(q)$. This behavior is recognized as the multifractal characteristic on the time axis. The temporal fluctuation is statistically self similar in the sense that temporally coarse-grained variables obey the

power laws (4.2) and in general, the scaling exponents $\tilde{\tau}_n(q)$ and $\tilde{\tau}_\epsilon(q)$ are nonlinear functions of q . The same kind of analysis as the present section has applied to the time series of an intermittent chaos in Ref. [24]. The time length where the above scaling behavior is expected to be observed is limited as $t_{min} \ll t \ll T$, where t_{min} and T are the smallest and largest characteristic times where the self-similarity in the above sense holds. Averaging over t for $t \gg T$ yields trivially the long-time average, and no power-law time dependence exists. The scaling laws as Eq. (4.2) thus hold for t less than the correlation time scale where the scaling $\langle \epsilon(t)\epsilon(0) \rangle \sim \epsilon_0^2 t^{\tilde{\tau}_\epsilon(2)}$ holds. One should notice that the exponent that characterizes the correlation decay is identical to $\tilde{\tau}_\epsilon(2)$ given in Eq. (4.2).

In addition to the scaling exponents in Eq. (4.2), one may consider the rate function of time scaling as follows. Let us define the local exponent \tilde{z}_ϵ and its rate function for the coarse-grained energy dissipation rate by

$$\epsilon_t = \epsilon_0 \left(\frac{T}{t} \right)^{\tilde{z}_\epsilon}, \quad \tilde{z}_\epsilon = \frac{\log \epsilon_t / \epsilon_0}{\log T/t}, \quad (4.3)$$

$$\tilde{S}_\epsilon(\tilde{z}) \sim - \frac{\log P_{\epsilon,t}(\tilde{z})}{\log T/t}, \quad (4.4)$$

where $P_{\epsilon,t}(\tilde{z})$ is the PDF of \tilde{z}_ϵ and T is the largest time scale of the system. By repeating a similar calculation in Sec. II, the concavity assumption on $\tilde{S}_\epsilon(\tilde{z})$ leads to the relation between the time scaling exponent and $\tilde{S}_\epsilon(z)$ for $t \ll T$ as

$$\tilde{\tau}_\epsilon(q) = \min_z [\tilde{S}_\epsilon(z) - qz]. \quad (4.5)$$

Similarly, the rate function $\tilde{S}_n(\tilde{z})$ is defined for the coarse-grained energy flux $|F_n|_t$.

To numerically check the power-law scaling of Eq. (4.2), the third- and fourth-order moments are shown in Fig. 8 for several inertial range energy fluxes and the energy dissipation rate for illustration. Power-law behavior (4.2) is observed over three decades. For higher shell, scaling regions tend to be wider in small time scales because the dynamics becomes faster and the inner cutoff time scale t_{min} becomes smaller.

The time scaling exponents numerically determined are plotted in Fig. 9. It is difficult to obtain statistical convergence of moments $\langle |F_n|^q \rangle$ and $\langle \epsilon_t^q \rangle$ for large $q (> 4)$. We discuss the converged data for $q < 4$ in Fig. 9. The data for $4 < q < 6$ in Fig. 9 are computed for another discussion made later. By definition, $\tilde{\tau}_n(q)$ and $\tilde{\tau}_\epsilon(q)$ vanish at both $q=0$ and 1. Comparing $\tilde{\tau}_n(q)$ with $\tilde{\tau}_\epsilon(q)$, one finds the difference of statistics between the inertial range energy flux and the energy dissipation rate. In a small- q region, the $\tilde{\tau}_\epsilon(q)$ curves more loosely near $q=0$ than $\tilde{\tau}_n(q)$'s (Fig. 10, the magnification of a small- q range of Fig. 9), and in a large- q region $\tilde{\tau}_\epsilon(q)$ goes above $\tilde{\tau}_n(q)$ (Fig. 9). To qualify these differences of temporal fluctuations, we calculated some characteristic

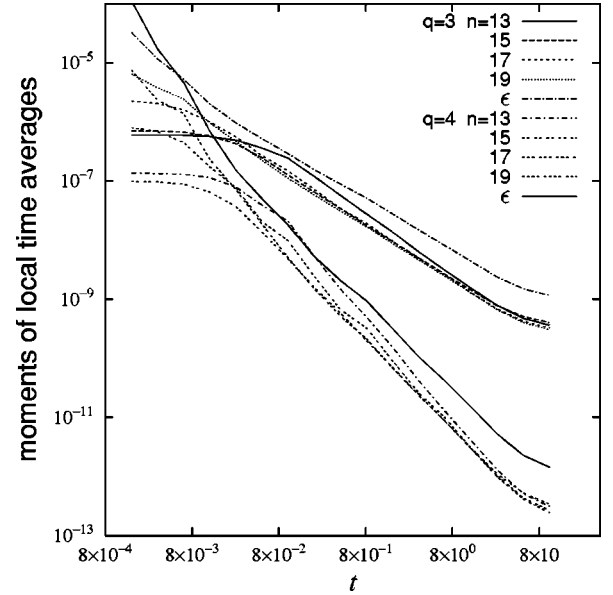


FIG. 8. The third and fourth moments of finite time average of the energy flux in the inertial range and the energy dissipation rate for run 4. The third moments are the upper lines and the fourth moments are the lower lines.

quantities. For a small- q region, the first and second derivatives at $q=0$ are important parameters since they determine the parabolic shapes of \tilde{S}_n and \tilde{S}_ϵ near their minima; one may make a qualitative comparison with these parameters (see Sec. III A). They are noted as $\tilde{z}_n(0) = -\tilde{\tau}_n'(0)$ (similar to Eq. (2.7)), and $\tilde{\tau}_n''(0)$, and the corresponding numerical values determined by the mean and the variance of \tilde{z} are

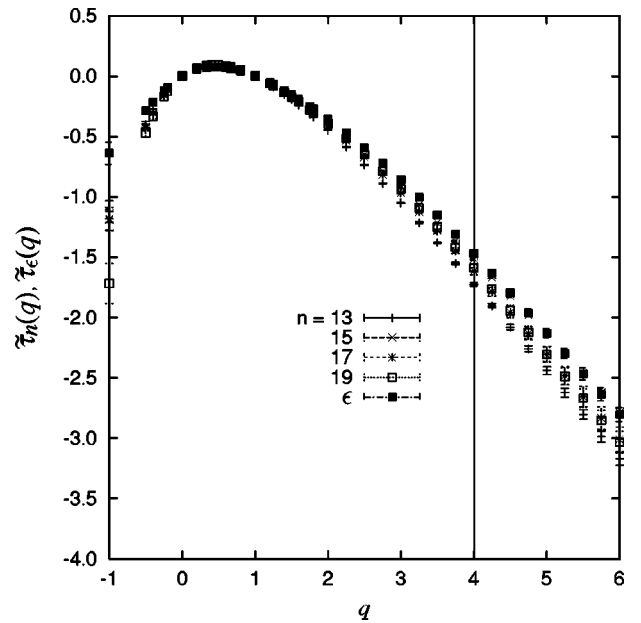


FIG. 9. The time scaling exponents $\tilde{\tau}_n(q)$ for the energy flux in the inertial range $n=13, 15, 17, 19$, and $\tilde{\tau}_\epsilon(q)$ for the energy dissipation rate for run 4. Moments, $\langle |F_n|^q \rangle$ and $\langle \epsilon_t^q \rangle$, are converged for $q < 4$. The error bars are given to the data.

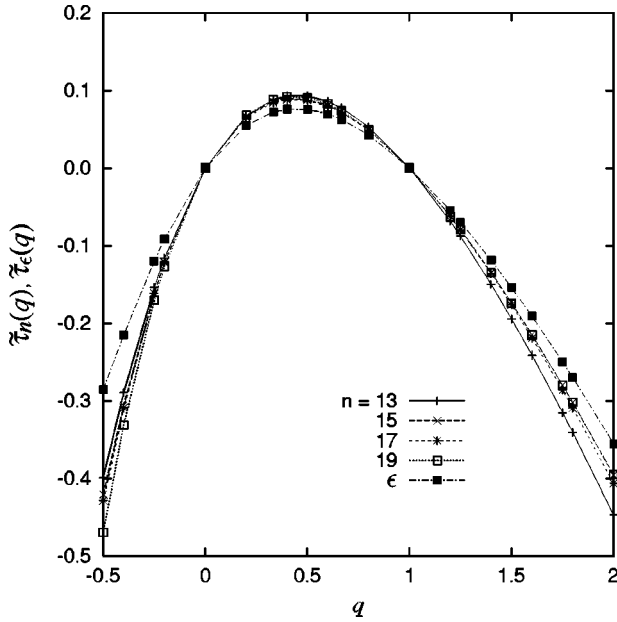


FIG. 10. Same data of $\tilde{\tau}_n(q)$ and $\tilde{\tau}_\epsilon(q)$ as in Fig. 9 shown in a smaller range of q values. Even in a small- q range, the statistics of the energy flux and the energy dissipation rate differ from each other.

given in Table II. The $\tilde{z}_n(0)$'s for the energy fluxes take approximately same values and are larger than $\tilde{z}_\epsilon(0)$ of the energy dissipation rate. Moreover, the $|\tilde{\tau}_n''(0)|$'s take larger values than $|\tilde{\tau}_\epsilon''(0)|$. The larger $|\tilde{z}_n(0)|$ and $|\tilde{\tau}_n''(0)|$ make $\tilde{\tau}_n(q)$ more tightly curving around $q=0$. This is a qualitative difference of the small fluctuation between the energy flux and the energy dissipation rate fluctuations.

The behavior of characteristic functions $\tilde{\tau}_n$ and $\tilde{\tau}_\epsilon$ for $q \rightarrow \infty$ is dominated by the strongest fluctuation in sample data, its corresponding exponent z being denoted as $\gamma (=z_{max}$ defined in Sec. II). γ values for $|F_n|_t$ and ϵ_t may be possibly determined as the intrinsic values of their fluctuations, or as the maximum order of events in finite sample data. Moreover, $q(\gamma)$ ($=q_{max}$ defined in Sec. II) is the maximum value of q of the convergence of moments. Whenever exponents of moments such as $\tau(q)$ are computed for $q > q(\gamma)$, one always observes the linear q dependence of a scaling exponent in a large- q region (cf. Sec. II). In this q region, $\tau(q)$ relates with $S(z)$ as $\tau(q) = -\gamma q + S(\gamma)$, γ and $S(\gamma)$ are constants

TABLE II. Characteristic parameters for the time scaling of the energy flux in the inertial range and the energy dissipation rate for run 4.

n	$\tilde{z}_n(0), \tilde{z}_\epsilon(0)$	$ \tilde{\tau}_n''(0) , \tilde{\tau}_\epsilon''(0) $	$\tilde{\gamma}_n, \tilde{\gamma}_\epsilon$
13	-0.46	1.40	0.73
15	-0.48	1.60	0.64
17	-0.47	1.58	0.70
19	-0.49	1.73	0.73
ϵ	-0.41	1.24	0.68

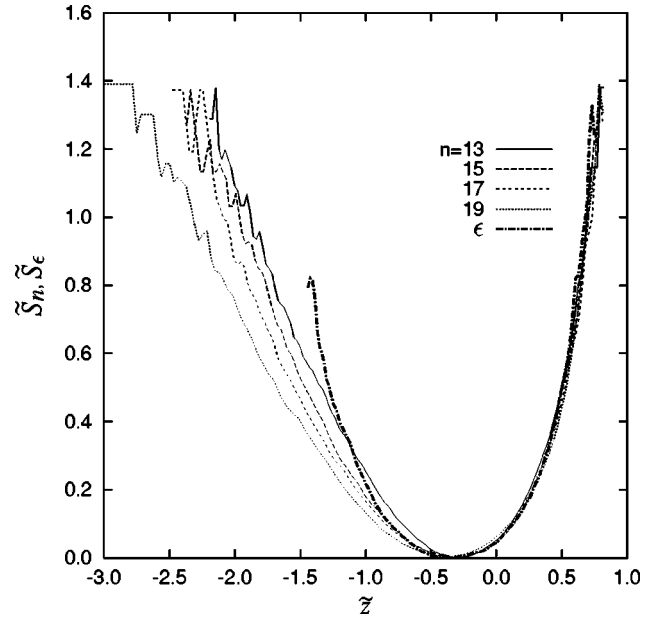


FIG. 11. Rate functions $\tilde{S}_n(\tilde{z})$ of the finite time-averaged energy flux in the inertial range $n=13, 15, 17, 19$, and the energy dissipation rate for run 4.

observed in each measurement where there is no relevant event with $z > \gamma$. $\tau(q)$ in this range of q is not determined by a larger fluctuation than γ , but by the γ -order fluctuation. This fact provides a way of estimating γ . In this range of q , the scaling exponent $\tau(q)$ surely becomes linear on q (Fig. 9). Namely, γ may be taken out from a linear fitting of the scaling exponent $\tau(q)$ in $q > q(\gamma)$ range. Although it may be regarded meaningless to compute $\tau(q)$ in this range of q since statistical convergence of moments is not guaranteed, it contains the information on the fluctuation of $z = \gamma$, i.e., the maximum fluctuation in measurement (cf. Sec. II).

We compute the γ value of $\tilde{\tau}_n$ and $\tilde{\tau}_\epsilon$, denoting $\tilde{\gamma}_n$ and $\tilde{\gamma}_\epsilon$. $\tilde{\gamma}_n$ and $\tilde{\gamma}_\epsilon$ are the quantities that characterize large fluctuations of the energy flux and the energy dissipation rate. $\tilde{\gamma}_n$ and $\tilde{\gamma}_\epsilon$ are calculated as the slope of $5 < q < 6$, where $q(\gamma)$ values for $\langle |F_n|_t^q \rangle$ and $\langle \epsilon_t^q \rangle$ are about 4, which are estimated by the way described in Sec. II with the time scaling rate functions \tilde{S}_n and \tilde{S}_ϵ . The estimated $\tilde{\gamma}_n$ and $\tilde{\gamma}_\epsilon$ are summarized in Table II. The $\tilde{\gamma}_n$'s of the energy fluxes are larger than $\tilde{\gamma}_\epsilon$ of the energy dissipation rate. The energy flux exhibits stronger fluctuation than the energy dissipation rate. This is a qualitative difference of the large fluctuation between the energy flux and the energy dissipation rate.

Figure 11 shows the rate functions $\tilde{S}_n(\tilde{z})$ for the energy flux and $\tilde{S}_\epsilon(\tilde{z})$ for the energy dissipation rate for run 4. Concerning their right half of \tilde{z} regions, although \tilde{S}_n of the energy flux and \tilde{S}_ϵ of the energy dissipation rate similarly depend on \tilde{z} , the rightmost point of \tilde{S}_ϵ is slightly smaller than that of \tilde{S}_n 's. The fluctuation of the energy flux is relatively larger than that of the energy dissipation rate. The differences of fluctuation natures between the energy flux and energy dissipation rate are thus observed through the time scal-

ing exponents and the corresponding rate functions.

What properties of energy transferring process do these differences produce? The difference of temporal intermittency between the energy flux and the energy dissipation is observed in the time scaling exponents or the rate functions, and is particularly qualified by the parameters $\tilde{z}_n(0)$, $\tilde{\tau}_n''(0)$ and $\tilde{\gamma}_n$. These differences of temporal intermittency are explained as follows. The energy dissipation rate is non-negative and always dissipates the energy. On the other hand, the energy flux is not always positive and may take negative values, and negative energy flux represents the inverse energy cascade. Their long-time averages are almost the same because of the stationarity of the energy cascade process. Therefore, the energy flux may take larger fluctuations than the energy dissipation rate. This fact makes $\tilde{\gamma}_n$ larger than $\tilde{\gamma}_\epsilon$. Furthermore, since $|\tilde{\tau}_n''(0)|$ and $|\tilde{\tau}_\epsilon''(0)|$ are related to the variances of scaling exponents and represents the fluctuation around the mean values, it is understood that $|\tilde{\tau}_n''(0)|$ is larger than $|\tilde{\tau}_\epsilon''(0)|$. The existence of the inverse energy cascade in the inertial range makes the inertial range intermittency different from that in the dissipation range.

Next, we consider the interrelation between the inertial range scaling and the time scaling of the energy flux. On the one hand, the inertial range scaling of the energy flux is defined as

$$\frac{|F_n|}{\langle |F_n| \rangle} = \left(\frac{k_n}{k_0} \right)^z, \quad (4.6)$$

with an instantaneous scaling exponent z . On the other hand, the time scaling is written as

$$\frac{t^{-1} \int_0^t |F_n(s)| ds}{\langle |F_n| \rangle} = \left(\frac{T}{t} \right)^{\tilde{z}_n}, \quad (4.7)$$

with a local scaling exponent \tilde{z}_n for $t_n < t < T$, where t_n is the inner scale of the time scaling associated with the n th shell. To discuss the connection between z and \tilde{z}_n , we take $t = t_n$ and approximate the integral in Eq. (4.7) as

$$\frac{1}{t_n} \int_0^{t_n} |F_n(s)| ds \sim |F_n(u)|, \quad (4.8)$$

with a time u in between 0 and t_n . Combining Eqs. (4.7) and (4.8), and comparing it with Eq. (4.6) yield

$$\left(\frac{T}{t_n} \right)^{\tilde{z}_n} \sim \left(\frac{k_n}{k_0} \right)^z. \quad (4.9)$$

We assume here that t_n is estimated by the natural turnover time

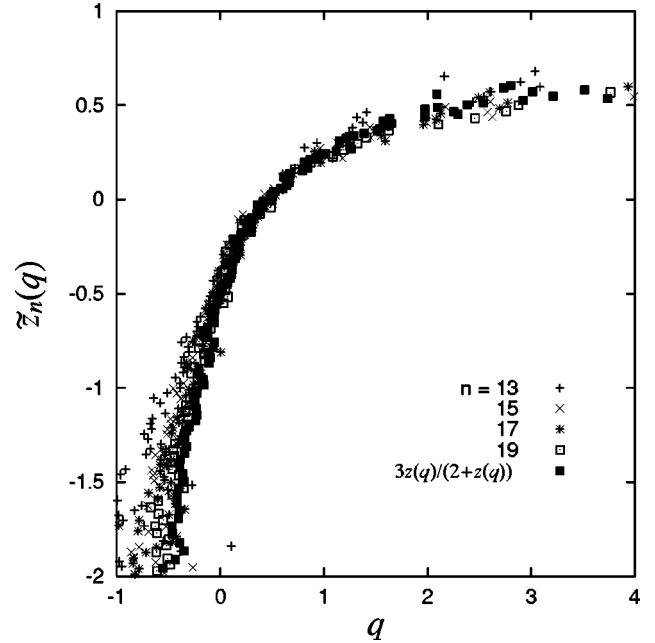


FIG. 12. $\tilde{z}_n(q)$ of time scaling and comparison with $z(q)$ of the inertial range scaling by the relation (4.11).

$$t_n \sim \frac{1}{k_n |u_n|} \sim \frac{1}{k_n^{2/3} |F_n|^{1/3}} \sim k_n^{-(2/3+z/3)}, \quad (4.10)$$

where the relation $|F_n| \sim k_n |u_n|^3$ has been used. This implies that t_n is a fluctuating time associated with z . From Eqs. (4.9) and (4.10), one obtains a relation

$$\tilde{z}_n = \frac{3z}{2+z}, \quad (4.11)$$

which states that $\tilde{S}_n(3z/2+z) = S(z)$. The minima $\tilde{S}_n = S = 0$ coincides with $\tilde{S}'_n = S' = 0$, thus for $q = 0$,

$$\tilde{z}_n(0) = \frac{3z(0)}{2+z(0)} \quad (4.12)$$

holds. For $\tilde{q}, q \rightarrow \infty$ of $\tilde{z}_n(\tilde{q})$ and $z(q)$, $\tilde{S}_n(\tilde{\gamma}_n) = S(\gamma)$, and therefore

$$\tilde{\gamma}_n = \frac{3\gamma}{2+\gamma}. \quad (4.13)$$

Using the observed values $z(0) = -0.28$ and $\gamma = 0.625$, the corresponding time exponents are calculated as $\tilde{z}_n(0) = -0.48$ and $\tilde{\gamma}_n = 0.714$. These values are compared to the observed data in Table II. They show a good agreement with each other except for $\tilde{\gamma}_{15}$. The disagreement for $\tilde{\gamma}_{15}$ may be due to the statistical inconvergence of data. Figure 12 shows

$\tilde{z}_n(q)$ with $3z(q)/[2+z(q)]$. This ensures the validity of the relation (4.11). The energy flux time scaling is thus linked to the multifractal behavior in the inertial range.

V. CONCLUDING REMARKS

In the present paper, we have discussed the characterization of the anomalous scaling of turbulence using the large deviation rate function.

We have computed the rate function $S(z)$ of the energy-flux fluctuation for the inertial range of the GOY model, and found the existence of the concave function $S(z)$. The anomalous exponents so far studied [15] implied the distribution of scaling exponents. This concavity property of the rate function proves that the rate function and structures function exponents, such as $\zeta(q)$ and $\tau(q)$, are related with each other by the Legendre transformation. Moreover, the rate function is found to be independent of the Reynolds number. For small fluctuation, the rate function is well approximated by the parabolic form, that is, near the minimum position of $S(z)$. On the other hand, for large fluctuation the observed $S(z)$ turns out to be in good agreement with that defined by the She-L ev eque model.

In the intermediate dissipation range, the viscous effect changes the form of the rate function, and we considered how the rate function is affected by the viscous effect in the intermediate dissipation range (IMDR). The rate function $S_n(z)$ partially coincides with the inertial range $S(z)$ in the large fluctuation range of z , which means that the inertial range scaling partially holds even at the crossover scale where viscous effect starts to affect. The cutoff exponent is used to quantify the IMDR scaling and its cutoff scale dependence was studied. This result confirms that the IMDR scaling is due to the multifractal characteristics in the inertial

range, in other words, to the fluctuation of viscous cutoff scale. Although, so far, several studies tried to verify the existence of the IMDR scaling by analyzing structures functions, they could not clearly observe it. In contrast to this preceding analysis, the rate function succeeds in quantifying the IMDR scaling. Experimental study to clarify the existence of the function $S_n(z)$ near the dissipation scale in real turbulent flow is highly desired.

Furthermore, we compared the intermittency statistics of the energy flux with those of the energy dissipation rate with the time scaling exponents in order to compare the intermittency characteristics in the inertial range and the dissipation range. This manner to characterize the intermittency is based on the long-time correlations of fluctuation. The result reveals the difference of intermittency between the energy flux and the energy dissipation rate, which is not only for the strong fluctuation but for weak fluctuation. This difference reflects the difference of the inertial range and the dissipation range dynamics, i.e., the difference of the energy transferring dynamics.

The self similarity of intermittent energy cascade is well characterized by the rate-function $S(z)$, and moreover the intermediate dissipation range scaling is observed also by the rate function. The rate function is a direct measure of the distribution of the scaling exponent and fundamental to study the intermittency problem. It is highly desired to apply the present rate-function approach to clarify the overall statistics of turbulent flows in experiments and observations.

ACKNOWLEDGMENTS

This study was partially supported by Grant-in-Aide for Scientific Research No.11837009 from the Ministry of Education, Science, Sports and Culture of Japan.

-
- [1] A.N. Kolmogorov, Dokl. Akad. Nauk SSSR **30**, 9 (1941).
 - [2] F. Anselmet, Y. Gagne, E.J. Hopfinger, and R.A. Antonia, J. Fluid Mech. **140**, 63 (1984).
 - [3] A.M. Oboukhov, J. Fluid Mech. **13**, 77 (1962); A.N. Kolmogorov, *ibid.* **13**, 82 (1962); A. S. Monin and A. M. Yaglom, *Statistical Fluid Mechanics* (MIT Press, Cambridge, MA, 1975); A.S. Gurvich and A.M. Yaglom, Phys. Fluids Suppl. **10**, S59 (1967).
 - [4] C. Meneveau and K.R. Sreenivasan, J. Fluid Mech. **224**, 429 (1991).
 - [5] R. Badii and P. Talkner, Phys. Rev. E **59**, 6715 (1999).
 - [6] I. Hosokawa, S. Oide, and K. Yamamoto, Phys. Rev. Lett. **77**, 4548 (1996).
 - [7] E.B. Gledzer, Dokl. Akad. Nauk SSSR **209**, 1046 (1973) [Sov. Phys. Dokl. **18**, 216 (1973)]; M. Yamada and K. Ohkitani, J. Phys. Soc. Jpn. **56**, 4210 (1987); K. Ohkitani and M. Yamada, Prog. Theor. Phys. **81**, 329 (1989).
 - [8] U. Frisch, *Turbulence* (Cambridge University Press, Cambridge, England, 1995).
 - [9] J.L. Gilson and T. Dombre, Phys. Rev. Lett. **79**, 5002 (1997).
 - [10] H. Fujisaka and S. Grossmann, Phys. Rev. E **63**, 026305 (2001).
 - [11] H. Fujisaka and M. Inoue, Prog. Theor. Phys. **77**, 1334 (1987); H. Fujisaka, *Statistical Mechanics in Nonequilibrium Systems* [in Japanese] (Sangyo-Tosho, Tokyo, 1998).
 - [12] D. Fukayama, T. Oyamada, T. Nakano, T. Gotoh, and K. Yamamoto, J. Phys. Soc. Jpn. **69**, 701 (2000).
 - [13] T. Watanabe, Y. Nakayama, and H. Fujisaka, Phys. Rev. E **61**, R1024 (2000).
 - [14] T. Bohr, M. Jensen, G. Paladin, and A. Vulpiani, *Dynamical Systems Approach to Turbulence* (Cambridge University Press, Cambridge, England, 1998).
 - [15] M.H. Jensen, G. Paladin, and A. Vulpiani, Phys. Rev. A **43**, 798 (1991); D. Pisarenko, L. Biferale, D. Courvoisier, U. Frisch, and M. Vergassola, Phys. Fluids A **5**, 2533 (1993); L. Kadanoff, D. Lohse, J. Wang, and R. Benzi, Phys. Fluids **7**, 617 (1995).
 - [16] U. Frisch and M. Vergassola, Europhys. Lett. **14**, 439 (1991).
 - [17] U. Frisch, Z.-S. She, and O. Thual, J. Fluid Mech. **168**, 221 (1986).
 - [18] Z.-S. She and E. L ev eque, Phys. Rev. Lett. **72**, 336 (1994).
 - [19] E. L ev eque and Z.-S. She, Phys. Rev. E **55**, 2789 (1997).
 - [20] B. Dubrulle, Phys. Rev. Lett. **73**, 959 (1994); Z.-S. She and

- E.C. Waymire, *ibid.* **74**, 262 (1995).
- [21] T. Watanabe and H. Fujisaka, J. Phys. Soc. Jpn. **69**, 1672 (2000).
- [22] E.A. Novikov, Dokl. Akad. Nauk SSSR **184**, 1072 (1969) [Sov. Phys. Dokl. **14**, 104 (1969)]; E.A. Novikov, Appl. Math. Mech. **35**, 231 (1971).
- [23] G. Paladin and A. Vulpiani, Phys. Rev. A **35**, 1971 (1987).
- [24] H. Fujisaka, H. Suetani, and T. Watanabe, Prog. Theor. Phys. Suppl. **139**, 70 (2000).